Optical Mouse Array Position Calibration for Mobile Robot Velocity Estimation

Sungbok Kim and Sanghyup Lee
Department of Digital Information Engineering
Hankuk University of Foreign Studies
Yongin-si, Gyoungi-do, 449-791, KOREA
{sbkim, toto718}@hufs.ac.kr

***Abstract*—This paper presents the position calibration of a polygonal array of optical mice for improved mobile robot velocity estimation using optical mice. First, the least squares velocity estimate of an omnidirectional mobile robot is obtained as the simple average of the velocity measurements from optical mice. Second, the sensitivity of the least squares velocity estimation to an imprecisely installed optical mouse array is analyzed. Third, with the aid of other accurate sensors, for example, wheel encoders, a simple but effective calibration for imperfect optical mouse array position is proposed. Finally, the position calibration of a regular triangular optical mouse array is given to demonstrate the effectiveness of the proposed method.**

***Keywords*—Mobile robot, velocity estimation, optical mouse, sensitivity analysis, position calibration**

I. INTRODUCTION

Personal service robots are expected to come into human daily life as supporters in education, leisure, house care, health care, and so on. Most of them built on a mobile platform require the capability of autonomous navigation in unknown and/or dynamic environments. The key ingredients for autonomous navigation are viable techniques for the map building, the obstacle detection/avoidance, and the localization in terms of velocity and position. The concern of this paper is the robust velocity estimation of an omnidirectional mobile robot as a platform of personal service robots.

There have been several attempts to employ the optical mice for the velocity estimation of a mobile robot [1-6]. In fact, the optical mouse is an inexpensive but high performance device with sophisticated image processing engine inside. The mobile robot velocity estimation using a set of optical mice can overcome the limitations of typical sensors with ease. A few to mention, wheel slippage in wheel encoders, the line of sight in ultrasonic sensors, and heavy computation in cameras [7].

Optical mice can continue providing two relative displacements in both lateral and longitudinal directions, at a prespecified sampling rate. So, two linear velocity components experienced by an optical mouse can be readily computed. For the velocity estimation of an omnidirectional mobile robot, one and half optical mice are required theoretically to determine three velocity components. While two optical mice were used in most of previous research [1-5], the potential of more than two optical mice was investigated in [6]. For a regular polygonal array of optical mice, the least squares velocity estimation was proposed, which requires extremely simple computation and is robust to random measurement noises [6].

In this paper, we focus on the position calibration of an imprecisely installed optical mouse array for improved mobile robot velocity estimation. This paper is organized as follows. Section II obtains the least squares velocity estimation as the simple average. Section III analyzes the velocity estimation errors owing to imprecise optical mouse array installation. Section IV proposes a simple but effective position calibration for imperfect optical mouse array. A position calibration example is given in Section V. Finally, the conclusion is made in Section VI.

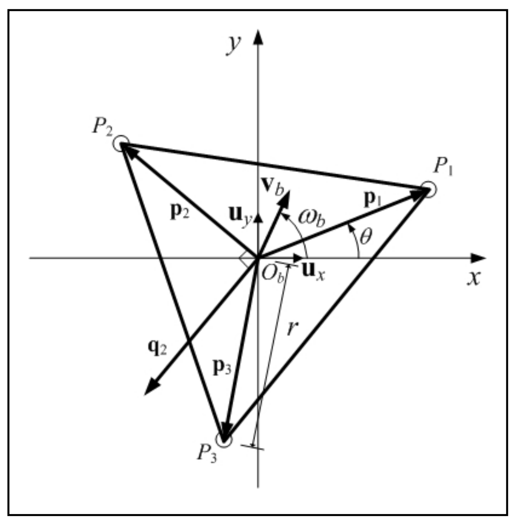

Figure 1. A regular triangular array of optical mice (N=3)

II. VELOCITY ESTIMATION

Assume that optical mice are installed at the vertices, P_i, $i=1,\cdots,N$, of a regular polygon that is centered at the center, O_b, of an omnidirectional mobile robot traveling on the xy plane. Fig. 1 shows an example of a regular triangular array of optical mice with $N=3$.

The optical mouse position vector, $\mathbf{p}_i = [\, p_{ix} \; p_{iy} \,]^t$, $i=1,\cdots,N$, from O_b to P_i, can be expressed as

978-1-4244-1676-9/08 /\$25.00 ©2008 IEEE RAM 2008

$$\mathbf{p}_i = \begin{bmatrix} p_{ix} \\ p_{iy} \end{bmatrix} = \begin{bmatrix} r\cos\{\theta + (i-1)\times\frac{2\pi}{N}\} \\ r\sin\{\theta + (i-1)\times\frac{2\pi}{N}\} \end{bmatrix} \quad (1)$$

where θ represents the heading angle of a mobile robot forwarding along the direction of $\mathbf{p}_1$, and r represents the distal distance of each optical mouse. For a regular polygonal arrangement of optical mice, we have

$$\sum_{i=1}^{N} p_{ix} = \sum_{i=1}^{N} p_{iy} = 0 \quad (2)$$

regardless of the heading angle θ.

Let υ_{bx} and υ_{by} be two linear velocity components and ω_b be the angular velocity component, all at the center O_b of an omnidirectional mobile robot. And, let υ_{ix} and υ_{iy}, $i = 1,\cdots,N,$ be two linear velocity components at the vertex P_i, which correspond to the velocity measurements from the i^{th} optical mouse. The velocity mapping from a mobile robot to an array of optical mice can be represented as [6]

$$\mathbf{A} \;\; \mathbf{v}_m = \mathbf{v}_s \quad (3)$$

where

$$\mathbf{v}_m = \begin{bmatrix} \upsilon_{bx} \\ \upsilon_{by} \\ \omega_b \end{bmatrix} \in \mathbf{R}^{3\times 1} \quad (4)$$

$$\mathbf{v}_s = \begin{bmatrix} \upsilon_{1x} \\ \upsilon_{1y} \\ \vdots \\ \upsilon_{Nx} \\ \upsilon_{Ny} \end{bmatrix} \in \mathbf{R}^{2N\times 1} \quad (5)$$

$$\mathbf{A} = \begin{bmatrix} 1 & 0 & -p_{1y} \\ 0 & 1 & p_{1x} \\ \vdots & \vdots & \vdots \\ 1 & 0 & -p_{Ny} \\ 0 & 1 & p_{Nx} \end{bmatrix} \in \mathbf{R}^{2N\times 3} \quad (6)$$

It should be noted that the Jacobian matrix $\mathbf{A}$ is a function of the positions of N optical mice, $\mathbf{p}_i$, $i = 1,\cdots,N$.

Typically, the velocity measurements from optical mice suffer from a certain amount of random noises. In the presence of random measurement noises, from (3), the least squares velocity estimation of a mobile robot can be obtained by

$$\mathbf{v}_m = \mathbf{B} \;\; \mathbf{v}_s \quad (7)$$

where

$$\mathbf{B} = (\mathbf{A}^t \mathbf{A})^{-1} \mathbf{A}^t \in \mathbf{R}^{3\times 2N} \quad (8)$$

Note that the lease squares estimation becomes equivalent to the maximum likelihood estimation when the measurement noises are independent and identically distributed zero-mean Gaussian variables [8].

Plugging (6) and (8) into (7) and applying (2) into the resulting equation, we obtain

$$\begin{aligned} \upsilon_{bx} &= \frac{1}{N}\sum_{i=1}^{N}\upsilon_{ix} \\ \upsilon_{by} &= \frac{1}{N}\sum_{i=1}^{N}\upsilon_{iy} \\ \omega_b &= \frac{1}{N}\sum_{i=1}^{N}\omega_i \end{aligned} \quad (9)$$

where

$$\omega_i = \frac{1}{r}\left[-\sin\{\theta + \frac{(i-1)\,2\pi}{N}\}\,\upsilon_{ix} + \cos\{\theta + \frac{(i-1)\,2\pi}{N}\}\,\upsilon_{iy}\right] \quad (10)$$

which represents the angular velocity experienced by the i^{th} optical mouse. Regarding the velocity estimation based on (9), the following remarks can be made. First, the angular velocity estimate ω_b, is dependent on the heading angle θ, unlike the linear velocity estimates, υ_{bx} and υ_{by}. Second, each of three velocity estimates is determined as the simple average of the corresponding velocity components read from all optical mice. Such computational simplicity is attributed to the arrangement of optical mice in a regular polygonal array centered at the center of a mobile robot.

The redundant number of optical mice helps to reduce the effect of random noises accompanying the velocity measurements from optical mice. Suppose that a mobile robot is commanded to travel at a constant linear velocity along the x axis, that is, $\upsilon_{bx} = \mu\,[\mathrm{m/sec}]$ with $\upsilon_{by} = 0.0\,[\mathrm{m/sec}]$ and $\omega_b = 0.0\,[\mathrm{rad/sec}]$. Then, the statistics of the optical mouse velocity measurements can be characterized by

$$\begin{aligned} E[\upsilon_{1x}] &= E[\upsilon_{2x}] = \cdots = E[\upsilon_{Nx}] = \mu \\ E[\upsilon_{1y}] &= E[\upsilon_{2y}] = \cdots = E[\upsilon_{Ny}] = 0 \end{aligned} \quad (11)$$

$$\begin{aligned} \mathrm{var}[\upsilon_{1x}] &= \mathrm{var}[\upsilon_{2x}] = \cdots = \mathrm{var}[\upsilon_{Nx}] = \sigma^2 \\ \mathrm{var}[\upsilon_{1y}] &= \mathrm{var}[\upsilon_{2y}] = \cdots = \mathrm{var}[\upsilon_{Ny}] = \sigma^2 \end{aligned} \quad (12)$$

where σ^2 represents the variance of each velocity measurement from N optical mice.

For the mobile robot velocity estimation based on (9), it can be shown that

$$E[\upsilon_{bx}] = \mu, \qquad E[\upsilon_{by}] = 0 \tag{13}$$

$$\mathrm{var}[\upsilon_{bx}] = \mathrm{var}[\upsilon_{by}] = \frac{\sigma^2}{N} \tag{14}$$

assuming that the velocity measurements from N optical mouse are independent each other. (14) tells that the greater the number of optical mice, the smaller the velocity estimation error, under the same level of measurement noises. Similar results to the above can be made for pure angular velocity and the combined linear and angular velocity of a mobile robot.

III. SENSITIVITY ANALYSIS

In practice, it may be rather difficult to install optical mice in an exact regular polygonal array centered at the center of a mobile robot. The sensitivity of the velocity estimation based on (9) to imprecise position installation of optical mice can be analyzed as follows. In the presence of installation error, the optical mouse position vector, $\tilde{\mathbf{p}}_i = [\,\tilde{p}_{ix} \;\; \tilde{p}_{iy}\,]^t, i = 1, \cdots, N$, can be described as

$$\tilde{\mathbf{p}}_i = \bar{\mathbf{p}}_i + \delta\mathbf{p}_i \tag{15}$$

where $\bar{\mathbf{p}}_i = [\,\bar{p}_{ix} \;\; \bar{p}_{iy}\,]^t$ represents the nominal mouse position, and $\delta\mathbf{p}_i = [\,\delta p_{ix} \;\; \delta p_{iy}\,]^t$ represents the deviation from the nominal value $\bar{\mathbf{p}}_i$. In what follows, we will use '¯'(bar), and '~'(tilde), to denote the nominal value and the perturbed value of the quantity of interest, respectively.

Taking into account imperfect optical mouse installation, the velocity kinematics, given by (3), can be expressed as

$$\tilde{\mathbf{A}} \; \tilde{\mathbf{v}}_m = \tilde{\mathbf{v}}_s \tag{16}$$

with

$$\tilde{\mathbf{v}}_m = \bar{\mathbf{v}}_m + \delta\mathbf{v}_m \tag{17}$$

$$\tilde{\mathbf{v}}_s = \bar{\mathbf{v}}_s + \delta\mathbf{v}_s \tag{18}$$

$$\bar{\mathbf{A}} = \bar{\mathbf{A}} + \delta\mathbf{A} \tag{19}$$

It should be noted that

$$\bar{\mathbf{A}} \; \bar{\mathbf{v}}_m = \bar{\mathbf{v}}_s \tag{20}$$

which is valid for the case of perfect optical mouse installation.

Premultiplying (16) by $\tilde{\mathbf{A}}^t$ and plugging (19) into the resulting equation, we have

$$(\bar{\mathbf{A}}^t + \delta\mathbf{A}^t)(\bar{\mathbf{A}} + \delta\mathbf{A})\,\tilde{\mathbf{v}}_m = (\bar{\mathbf{A}}^t + \delta\mathbf{A}^t)\,\tilde{\mathbf{v}}_s \tag{21}$$

Assuming that the optical mouse installation errors are sufficiently small enough,

$$\delta\mathbf{A}^t\,\delta\mathbf{A} \cong 0_{3\times3} \tag{22}$$

(21) becomes

$$(\bar{\mathbf{P}} + \delta\mathbf{P})\,\tilde{\mathbf{v}}_{\mathrm{m}} \cong (\bar{\mathbf{A}}^t + \delta\mathbf{A}^t)\,\tilde{\mathbf{v}}_{\mathrm{s}} \tag{23}$$

where

$$\bar{\mathbf{P}} = \bar{\mathbf{A}}^t\,\bar{\mathbf{A}} \in \mathbf{R}^{3\times3} \tag{24}$$

$$\delta\mathbf{P} = \delta\mathbf{A}^t\,\bar{\mathbf{A}} + \bar{\mathbf{A}}^t\,\delta\mathbf{A} \in \mathbf{R}^{3\times3} \tag{25}$$

Plugging (17) and (18) into (23), and applying (20) to the resulting equation, we obtain

$$\bar{\mathbf{P}}\,\delta\mathbf{v}_m + \delta\mathbf{P}\,\bar{\mathbf{v}}_m \cong \delta\mathbf{A}^t\,\bar{\mathbf{v}}_{\mathrm{s}} + \bar{\mathbf{A}}^t\,\delta\mathbf{v}_{\mathrm{s}} \tag{26}$$

under the additional assumptions of

$$\delta\mathbf{P}\,\delta\mathbf{v}_m \cong 0_{3\times1} \tag{27}$$

$$\delta\mathbf{A}^t\,\delta\mathbf{v}_s \cong 0_{3\times1} \tag{28}$$

Finally, from (26), the mobile robot velocity estimate error owing to imprecise optical mouse installation can be approximated by

$$\delta\mathbf{v}_m \cong \delta\mathbf{v}_{m,1} + \delta\mathbf{v}_{m,2} + \delta\mathbf{v}_{m,3} \tag{29}$$

where

$$\begin{aligned} \delta\mathbf{v}_{m,1} &= \bar{\mathbf{P}}^{-1}\,\delta\mathbf{A}^t\,\bar{\mathbf{v}}_{\mathrm{s}} \\ \delta\mathbf{v}_{m,2} &= -\bar{\mathbf{P}}^{-1}\,\delta\mathbf{P}\,\bar{\mathbf{v}}_m \\ \delta\mathbf{v}_{m,3} &= \bar{\mathbf{P}}^{-1}\,\bar{\mathbf{A}}^t\,\delta\bar{\mathbf{v}}_{\mathrm{s}} \end{aligned} \tag{30}$$

It should be noticed that the velocity estimation error is attributed to the mouse position deviation itself, $\delta\mathbf{A}$ and $\delta\mathbf{P}$, and the additional mouse measurements caused by the positional deviation, $\delta\mathbf{v}_{\mathrm{s}}$.

IV. POSITION CALIBRATION

A regular polygonal array of optical mice can provide the velocity estimation, which requires extremely simple computation and is robust to random measurement noises. However, imperfect optical mouse installation deviated from a regular polygon may deteriorate the accuracy of the resulting velocity estimation significantly. With the aid of other accurate sensors, the optical mouse installation errors can be readily calibrated. As an example, wheel encoders can provide very accurate velocity measurements under the environment of no wheel slippage.

Plugging (24) into (23) and rearranging the resulting equation, we have

$$\delta \mathbf{A}^t \, \tilde{\mathbf{v}}_s - \delta \mathbf{P} \, \tilde{\mathbf{v}}_m \;\cong\; \bar{\mathbf{A}}^t \, (\bar{\mathbf{A}} \, \tilde{\mathbf{v}}_m - \tilde{\mathbf{v}}_s) \tag{31}$$

With

$$\tilde{\mathbf{v}}_m = \begin{bmatrix} \tilde{\upsilon}_{bx} \\ \tilde{\upsilon}_{by} \\ \tilde{\omega}_b \end{bmatrix} \in \mathbf{R}^{3\times 1} \tag{32}$$

$$\tilde{\mathbf{v}}_s = \begin{bmatrix} \tilde{\upsilon}_{1x} \\ \tilde{\upsilon}_{1y} \\ \vdots \\ \tilde{\upsilon}_{Nx} \\ \tilde{\upsilon}_{Ny} \end{bmatrix} \in \mathbf{R}^{2N\times 1} \tag{33}$$

$$\delta \mathbf{A} = \begin{bmatrix} 0 & 0 & -\delta p_{1y} \\ 0 & 0 & \delta p_{1x} \\ \vdots & \vdots & \vdots \\ 0 & 0 & -\delta p_{Ny} \\ 0 & 0 & \delta p_{Nx} \end{bmatrix} \in \mathbf{R}^{2N\times 3} \tag{34}$$

it can be shown that

$$\delta \mathbf{A}^t \, \tilde{\mathbf{v}}_s = \mathbf{C}_1 \, \delta \mathbf{p} \tag{35}$$

$$-\delta \mathbf{P} \, \mathbf{v}_m = \mathbf{C}_2 \, \delta \mathbf{p} \tag{36}$$

where

$$\delta \mathbf{p} = \begin{bmatrix} \delta \mathbf{p}_1 \\ \vdots \\ \delta \mathbf{p}_N \end{bmatrix} \in \mathbf{R}^{2N\times 1} \tag{37}$$

$$\mathbf{C}_1 = \begin{bmatrix} 0 & 0 & \cdots & 0 & 0 \\ 0 & 0 & \cdots & 0 & 0 \\ \tilde{\upsilon}_{1y} & -\tilde{\upsilon}_{1x} & \cdots & \tilde{\upsilon}_{Ny} & -\tilde{\upsilon}_{Nx} \end{bmatrix} \in \mathbf{R}^{3\times 2N} \tag{38}$$

$$\mathbf{C}_2 = \begin{bmatrix} 0 & \tilde{\omega}_b & \cdots & 0 & \tilde{\omega}_b \\ -\tilde{\omega}_b & 0 & \cdots & -\tilde{\omega}_b & 0 \\ c_{11} & c_{12} & \cdots & c_{N1} & c_{N2} \end{bmatrix} \in \mathbf{R}^{3\times 2N} \tag{39}$$

with

$$\begin{aligned} c_{i1} &= -\tilde{\upsilon}_{by} - 2\,\tilde{\omega}_b \, p_{ix} \\ c_{i2} &= \tilde{\upsilon}_{bx} - 2\,\tilde{\omega}_b \, p_{iy} \end{aligned} \tag{40}$$

Plugging (35) and (36) into (31), we obtain

$$\mathbf{S}_k \, \delta \mathbf{p} \;\cong\; \mathbf{b}_k \tag{41}$$

where

$$\mathbf{S}_k = \mathbf{C_1} + \mathbf{C_2} \in \mathbf{R}^{3\times 2N} \tag{42}$$

$$\mathbf{b}_k = \bar{\mathbf{A}}^t \, (\bar{\mathbf{A}} \, \tilde{\mathbf{v}}_m - \tilde{\mathbf{v}}_s) \in \mathbf{R}^{3\times 1} \tag{43}$$

(41) represents a set of three equations obtained from the k^{th} measurement, in which $\delta \mathbf{p}$ is unknown, while both $\mathbf{S}_k$ and $\mathbf{b}_k$ are computed from $\bar{\mathbf{A}}$ (nominal value), $\tilde{\mathbf{v}}_m$ (estimated value by other accurate sensors), and $\tilde{\mathbf{v}}_s$ (measured value).

Aggregating the measurement equations resulting M from independent measurements, we can have

$$\mathbf{S} \, \delta \mathbf{p} \;\cong\; \mathbf{b} \tag{44}$$

with

$$\mathbf{S} = \begin{bmatrix} \mathbf{S}_1 \\ \mathbf{S}_2 (3,:) \\ \vdots \\ \mathbf{S}_M (3,:) \end{bmatrix} \in \mathbf{R}^{(M+2)\times 2N} \tag{45}$$

$$\mathbf{b} = \begin{bmatrix} \mathbf{b}_1 \\ \mathbf{b}_2 (3) \\ \vdots \\ \mathbf{b}_M (3) \end{bmatrix} \in \mathbf{R}^{(M+2)\times 1} \tag{46}$$

where $\mathbf{S}_k(3,:)$, $k = 2, \cdots, M$, is the 3^{rd} row vector of $\mathbf{S}_k$, and $\mathbf{b}_k(3)$, $k = 2, \cdots, M$, is the 3^{rd} element of $\mathbf{b}_k$. Seen from (38), (39), and (42), all the measurements other than the 1^{st} one can add only a single equation to $\mathbf{S}$.

Finally, from (44), the optical mouse array position error can be determined by

$$\delta \mathbf{p} \;\cong\; \mathbf{T} \, \mathbf{b} \tag{47}$$

where

$$\mathbf{T} = (\mathbf{S}^t \, \mathbf{S})^{-1} \, \mathbf{S}^t \in \mathbf{R}^{6\times 3M} \tag{48}$$

It can be shown that the necessary condition that $\mathbf{S}^t\,\mathbf{S}$ is invertible is given by

$$M \geq 2N - 2 \tag{49}$$

which tells that the number of independent measurements required for the optical mouse array position calibration should be at least $(2N-2)$.

V. EXAMPLE

Commercial optical mice used in our experiments have the ADNS-3080 [9], a high performance optical mouse sensor from the Agilent Technologies (now the Avago Technologies). Table Ⅰ shows the technical specifications and the parameter settings of the ADNS-3080. In stream mode, the optical mouse continues sending to the host the packet containing two relative displacements in both horizontal and vertical directions. Note that the relative displacement is internally expressed in the unit of counts, which needs to be converted in the unit of inches or meters for later use.

TABLE I. TECHNICAL SPECIFICATIONS AND PARAMETER SETTINGS OF THE ADNS-3080

	Unit	Specification	Parameter Setting
Frame Rate	fps (frames-per-sec)	500 ~ 6,469	6400
Resolution	cpi (counts-per-inch)	400 / 1,600	1,600
Maximum Speed	ips (inches-per-sec)	40 (@6,400fps)	40

To reduce communication overhead from the optical mouse to the host, we insert the downsampler implemented using ATmega8, 8-bit AVR microcontroller with 8K bytes in-system programmable flash from Atmel Corp. [10], as shown in Fig. 2.

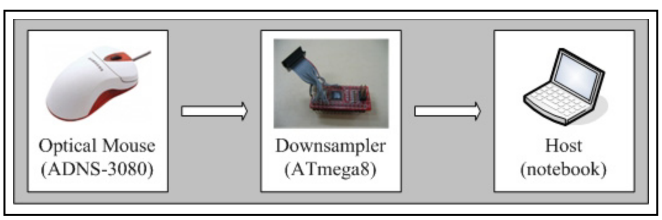

Figure 2. Optical mouse data acquisition system.

Upon receiving each packet from the host, the downsampler keeps on accumulating the relative displacement counts within the packet. Once every $K(=12)$ packets from the host, the downsampler sends to the host the packet containing the accumulated values of relative displacement accounts. Using these values, the host calculates the linear velocity components by, for example,

$$\upsilon_{ix} = \frac{\Delta x}{\Delta t} = \frac{\sum_{j=1}^{K} CNT_j / \mathrm{CPI}}{K / \mathrm{FPS}} \;[\mathrm{in/sec}] \tag{50}$$

where CNT_j, $j = 1, \cdots, K$, represents the relative displacement count of the j^{th} packet, and CPI represents the resolution in counts-per-inch; K represents the number of packets whose relative displacement is accumulated, and FPS represents the sampling rate in frames-per-sec.

For a regular triangular array of optical mice $(N = 3)$ shown in Fig. 1, with $r = 0.3$ [m] and $\theta = -\frac{\pi}{6}$ [rad], we set the nominal (wrong) optical mouse position, $\overline{\mathbf{p}}$, and the actual (true) optical mouse position, $\hat{\mathbf{p}}$, as follows:

$$\overline{\mathbf{p}} = 0.3 \times [0.866 \;\; -0.500 \;\; 0.000 \;\; 1.000 \;\; -0.866 \;\; -0.500]^t \tag{51}$$

$$\begin{aligned}\hat{\mathbf{p}} &= 1.05\,\overline{\mathbf{p}} \\ &= 0.3 \times [0.909 \;\; -0.525 \;\; 0.000 \;\; 1.050 \;\; -0.909 \;\; -0.525]^t\end{aligned} \tag{52}$$

It should be noticed that the actual optical mouse array is intentionally set to be slightly bigger than the actual one, as will be shown later.

A mobile robot equipped with the regular triangular optical mouse array described above is commanded to move in a constant speed self-rotation: $\upsilon_{bx} = \upsilon_{by} = 0.0$ [m/sec] and $\omega_b = \frac{1}{3}$ [rad/sec]. After taking ten independent measurements, that is, $M = 10$, we construct the measurement equation in the form of (44). Based on (47), the calibrated mouse position $\tilde{\mathbf{p}}$ was then found to be

$$\tilde{\mathbf{p}} = 0.3 \times [0.912 \;\; -0.526 \;\; 0.000 \;\; 1.053 \;\; -0.912 \;\; -0.526]^t \tag{53}$$

Comparing (53) with (52), one can see that the position calibration proposed in this paper works well under the presence of measurement noises, and the accuracy in position calibration is also highly satisfactory in spite of the simplicity of algorithm.

Next, let us evaluate the performance improvement in mobile robot velocity estimation attained as a result of the optical mouse array position calibration. Again, a mobile robot is commanded to move in a constant speed self-rotation: $\upsilon_{bx} = \upsilon_{by} = 0.0$ [m/sec] and $\omega_b = \frac{1}{3}$ [rad/sec]. For a given set of noisy optical mouse measurements, based on (9), the mobile robot velocity estimates ware computed under three different situations: 1) $\tilde{\mathbf{v}}_m$ after the mouse position calibration ($\mathbf{p} = \tilde{\mathbf{p}}$), 2) $\overline{\mathbf{v}}_s$ before mouse position calibration ($\mathbf{p} = \overline{\mathbf{p}}$), and 3) $\hat{\mathbf{v}}_m$ with accurate mouse position ($\mathbf{p} = \hat{\mathbf{p}}$). For 500 sampling intervals, Fig. 3 shows the plots of the mobile robot velocity estimates obtained under three different situations. From Fig. 3, the following observations can be made. First, the plot of $\tilde{\omega}_b$ is shifted downward compared to the plot of $\overline{\omega}_b$. This results

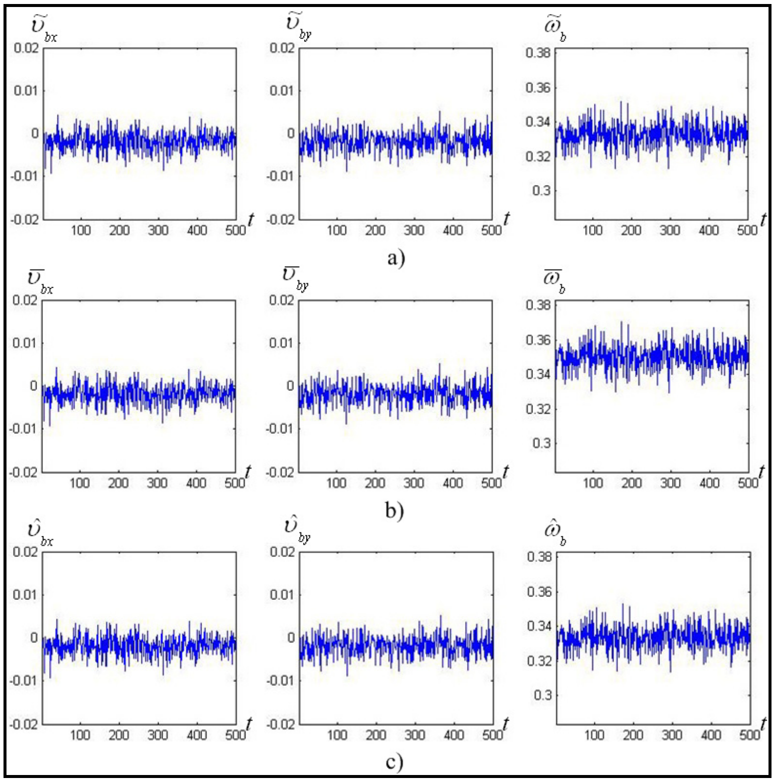

Figure 3. The mobile robot velocity estimates computed under three different situations: a) $\widetilde{\mathbf{v}}_m$ after position calibration, b) $\overline{\mathbf{v}}_m$ before position calibration, and c) $\hat{\mathbf{v}}_m$ with accurate position known a priori.

from the fact that the actual regular triangle of optical mice was set to be slightly bigger than the nominal position. Second, each of three plots of $\widetilde{\mathbf{v}}_m$ is almost the same as the corresponding plot of $\hat{\mathbf{v}}_m$, which demonstrates the accuracy of the proposed optical mouse array position calibration indirectly. Needless to say, the pattern of fluctuations (unbiased) is quite similar for each component of, $\widetilde{\mathbf{v}}_m$, $\overline{\mathbf{v}}_m$ and $\hat{\mathbf{v}}_m$, which captures the influence of random measurement noises. Above all, it should be mentioned that the accurate angular velocity estimate resulting from the optical mouse position calibration plays a critical role for the autonomous localization of a mobile robot.

VI. Conclusion

In this paper, we dealt with the position calibration of an imprecisely installed optical mouse array for improved mobile robot velocity estimation. The main contributions of this paper include 1) the least squares velocity estimation in the form of the simple average, 2) the sensitivity analysis to imperfect optical mouse array installation, and 3) a simple but effective position calibration of an optical mouse array. We hope that the results of this paper having notable simplicity and efficiency can facilitate the practical use of optical mouse based velocity estimation especially for personal service robots.

References

[1] D. K. Sorensen, V. Smukala, M. Ovinis, and S. Lee, "On-Line Optical Flow Feedback for Mobile Robot Localization/Navigation," Proc. IEEE Int. Conference on Intelligent Robots and Systems, 2003, pp. 1246-1251.

[2] S. Lee and J. Song, "Mobile Robot Localization Using Optical Flow Sensors," Int. J. Control, Automation, and Systems, vol. 2, no. 4, 2004, pp. 485-493.

[3] A. Bonarini, M. Matteucci, and M. Restelli, "A Kinematic-independent Dead-reckoning Sensor for Indoor Mobile Robotics," Proc. IEEE Int. Conference on Intelligent Robots and Systems, 2004, pp. 3750-3755.

[4] A. Bonarini, M. Matteucci, and M. Restelli, "Automatic Error Detection and Reduction for an Odometric Sensor based on Two Optical Mice," Proc. IEEE Int. Conference on Robotics and Automation, 2005, pp. 1687-1692.

[5] S. P. N. Singh and K. J. Waldron, "Design and Evaluation of an Integrated Planar Localization Method for Desktop Robotics," Proc. IEEE Int. Conference on Robotics and Automation, 2004, pp. 1109-1114.

[6] S. Kim and H. Kim, "Least Squares Velocity Estimation of a Mobile Robot Using a Regular Polygonal Array of Optical Mice," J. Control, Automation and Systems Eng., vol. 13, no. 10, 2007, pp. 978-982.

[7] J. Borenstein, H. R. Everett, L. Feng, Where am I?: Sensors and Methods for Mobile Robot Positioning, Dept. Mechanical Eng. Michigan University, 1996.

[8] Y. Bar-shalom, X. R. Li, and T. Kirubarajan, Estimation with Applications to Tracking and Navigation, John Wiley & Sons, Inc., 2001.

[9] ADNS-3080 High-Performance Optical Mouse Sensor Data Sheet, Avago Technologies, 2007.

[10] ATmega8 Data Sheet, Atmel Corp., 2007.